Reports

Native Iron in the Continental Lower Crust: Petrological and Geophysical Implications

Abstract. *Lower crustal granulite xenoliths recovered from a kimberlite pipe in western Africa contain native iron (Fe^0) as a decomposition product of garnet and ilmenite. Magnetic measurements show that less than 0.1 percent (by volume) of iron metal is present. Data from geothermometry and oxygen geobarometry indicate that the oxide and metal phases equilibrated between iron-wüstite and magnetite-wüstite buffers, which may represent the oxidation state of the continental lower crust, and the depleted lithospheric upper mantle. Ferromagnetic native iron could be stable to a depth of ≈95 kilometers and should be considered in the interpretation of long-wavelength static magnetic anomalies.*

STEPHEN E. HAGGERTY
PAUL B. TOFT
Department of Geology,
University of Massachusetts,
Amherst 01003

Information on the mineralogy of the deep continental crust is extremely limited (*1*), and the redox state of the lower crust has never been fully addressed. Although the earth's core is probably dominated by metallic iron, terrestrial conditions at the surface are generally oxidized. Naturally occurring iron metal, native iron, is rarely formed except in coal beds, low-temperature (<500°C) serpentinites, lavas that have or may have incorporated carbonaceous sediments (*2*), and, at one locality, in a quartz garnet glaucophane lawsonite assemblage (*3*).

We report the discovery of native iron in lower crustal granulites from Liberia in western Africa. The rocks (2 to 25 cm in diameter) were recovered from a diamond-bearing kimberlite pipe (10°41′W, 7°33′N) that erupted within the southern shield of the West African craton in the mid-Cretaceous, 90 to 120 million years ago after the breakup of Gondwanaland (*4*). Granulites and other xenoliths were incorporated from the walls of the volcanic conduit into the kimberlite on its upward passage from the mantle. Although high temperatures were attained, rapid adiabatic cooling has prevented thermal metamorphism of the xenoliths or chemical interaction with the kimberlite.

The granulites, composed of 1- to 5-mm garnet, clinopyroxene, and plagioclase with accessory ilmenite and rutile, are similar to granulites found elsewhere in Africa (*5*) and other parts of the world (*6*). Garnet-pyroxene geothermometry (*7*) yields equilibration temperatures of 700° to 780°C based on a lower crustal pressure of 10 kbar, commensurate with temperatures and pressures of granulite facies metamorphism. Partial melting in some granulites has produced second-generation pyroxene with kyanite and scapolite, and these rocks record temperatures well above 800°C. Rutile is overgrown by Fe^{2+}-freudenbergite ($Na_2FeTi_7O_{16}$), which is sodium-metasomatic in origin (*8*), derived from reaction with a fluid phase also enriched in calcium, sulfur, and CO_2 (and possibly CO and CH_4) that crystallized interstitial scapolite (*9*) and pervasive sulfides (troilite, pentlandite, and chalcopyrite); rare graphite formed along cracks and mineral grain boundaries.

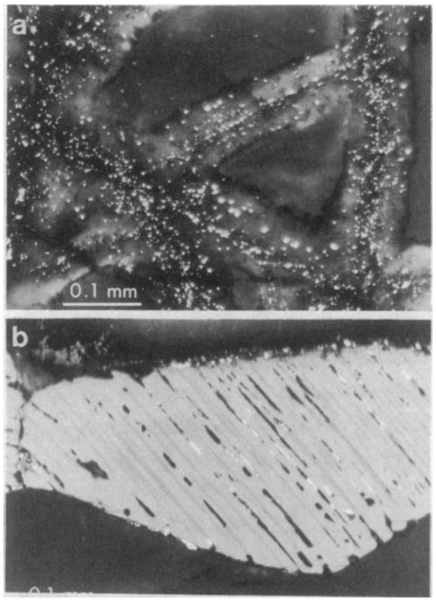

Fig. 1. Reflected-light photomicrographs of native iron-bearing assemblages obtained with a ×20 oil-immersion objective. (a) Garnet decomposition along cracks to metallic iron (bright, white spheres) in association with scapolite + tschermakitic amphibole. (b) Ilmenite grain, set in clinopyroxene, that has undergone subsolidus reduction to lamellar ulvöspinel (dark gray laths) + iron metal (bright white); the black laths are plucked areas from sample preparation.

Garnets are Fe^{2+}-rich with 51 to 56 mole percent almandine ($Fe_3Al_2Si_3O_{12}$), 27 to 32 percent pyrope ($Mg_3Al_2Si_3O_{12}$), and 14 to 17 percent grossular ($Ca_3Al_2Si_3O_{12}$). Incipient to advanced decomposition has produced iron metal particles (<2 to ≈10 μm), partially or completely enveloped in magnetite. Metal and oxide assemblages are concentrated along crystal edges and in irregular fracture patterns throughout garnets (Fig. 1a). Electron microbeam analyses show that the metal is composed of 98 to 99 percent (by weight) iron, with minor nickel (≈0.15 percent), cobalt (≈0.35 percent), copper (≈0.3 percent), and zinc (≈0.2 percent). The matrix to native iron is a spongy, fine-grained, white, translucent phase identified in some cases as scapolite; in other samples it remains unidentified. A highly aluminous (18 to 21 percent Al_2O_3) tschermakitic amphibole, assumed to be of high-pressure origin (*10*), is also present. Experiments (*11*) indicate that almandine garnet is unstable at oxygen fugacities (fO_2) above the FMQ (fayalite = magnetite + quartz) buffer at 2 kbar and at temperatures above ~850°C. Although higher pressures increase the thermal stability, we know of no experimental data for garnets of the present compositions.

Native iron also resulted from the decomposition of ilmenite (Fig. 1b). The assemblage is ilmenite ($FeTiO_3$) + ulvöspinel (Fe_2TiO_4) ± iron (Fe^0), with troilite (FeS) as an accessory phase. The iron in this assemblage has grain sizes similar to those of the iron particles in garnet but lower contents of nickel, cobalt, copper, and zinc (total of <0.5 percent). Very low concentrations of Fe^{3+} in both the ulvöspinels (0.2 to 0.3 percent Fe_2O_3) and ilmenites (0.1 to 2.4 percent) are consistent with experimental data (*12*) for iron-titanium oxides in equilibrium with metallic iron; these findings suggest that the ilmenite decomposed at ≈1000°C at low fO_2 (<IW, iron-wüstite) and that the ulvöspinel may be cation-deficient and titanium-rich. Applying the solution parameter model for metal-free, coexisting iron-titanium ox-

ides (*13*), we obtained equilibration temperatures for these oxides of 996° to 830°C at fO_2 between $10^{-12.2}$ and $10^{-16.2}$ atm. These data correspond to conditions just above the MW (magnetite-wüstite) buffer at 1 bar and between MW and IW if the buffers are corrected to a total pressure of 10 kbar.

On the basis of the textural relations of the iron metal in garnet and ilmenite and the differences in temperature obtained from garnet-clinopyroxene and ilmenite-ulvöspinel mineral thermometers, we suggest that native iron formed in the solid state at higher temperatures than those implied from iron-magnesium and calcium exchange in the silicates. If pressures greater than 10 kbar prevailed, then higher temperatures would result. We conclude that decomposition was initiated below IW and equilibrated to IW–MW. Native iron was formed at high temperatures (≃800° to 1000°C) and decomposition was induced at high pressures (≃10 kbar), on the basis of the assemblage scapolite, tschermakitic amphibole, and Fe^{2+}-freudenbergite.

Selected physical properties of the larger specimens of granulites are listed in Table 1. Apparent specific gravities range from 2.75 to 3.25, but most values are between 2.95 and 3.25. Equating specific gravity to density, on the basis of Birch's relationship for granulites (*14*) as modified by temperature (*15*) we estimate compressional seismic wave velocities (V_p) of 6.3 to 7.2 km sec^{-1}.

Curie balance thermomagnetic analyses (*16*) of several specimens confirmed the presence of iron metal and magnetite. Each analysis (≃10-mg chips from samples 3, 4, 9, and 25) showed reversible magnetic transitions at 580° and 770°C (± 25°C), the Curie temperatures of pure magnetite and pure iron, respectively.

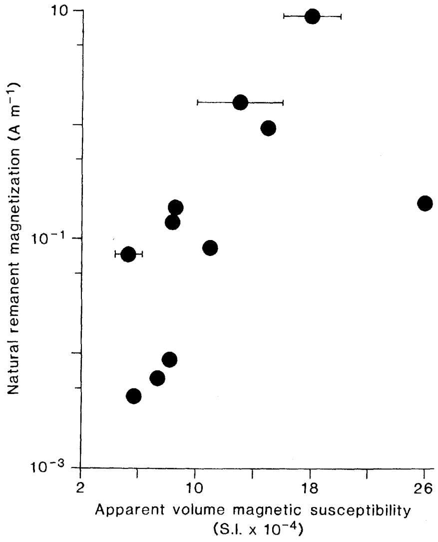

Fig. 2. Relation of natural remanent magnetization to apparent magnetic susceptibility per unit volume (X_v) for lower crustal granulites (from Table 1).

The magnetic susceptibility per unit volume (X_v) of the granulites at room temperature and pressure is 0.5×10^{-3} to 3×10^{-3} [S.I. (Système International d'Unités)], the natural remanent magnetization (NRM) intensities range from about 10^{-3} to 10 A m^{-1}, and the Königsberger ratio (Q) is usually >1 (Table 1). Figure 2 suggests a proportional relation between the restricted values of magnetic susceptibility and the wide range of NRM intensity.

Long-wavelength (50 to 500 km) aeromagnetic anomalies and magnetic anomalies derived from POGO (Polar Orbiting Geophysical Observatory) and MAGSAT (Magnetic Field Satellite) satellite measurements frequently appear to require lower crustal magnetic sources with contrasts in magnetization intensity in excess of 1 A m^{-1} (*17*), a range of induced magnetization rarely attained on a large areal scale by dominant crustal materials exposed at the earth's surface (*18*). Magnetite-bearing granulites are considered the most probable source rocks (*17, 19*), particularly if thermally promoted viscous magnetic remanence (*20*) or the Hopkinson effect of thermally enhanced susceptibility [≃×2 for magnetite (*21*)] is considered, but metal alloys in the upper mantle also have been suggested as possible mineral magnetic sources (*22*).

Table 1. Magnetic properties and specific gravities of lower crustal granulites.

Sample No.*	Apparent specific gravity	X_v† (× 10^{-4})	NRM‡ (A m^{-1})	J§ (A m^{-1} × 10^{-2})	Q‖	M¶ (A m^{-1})
1	3.12	26	0.21	6.5	3.2	0.28
3	2.75	7.4	0.0062	1.8	0.34	0.024
4	3.21	13 (± 3)	1.6	3.2	50	1.6
7	3.02	8.2	0.009 (± 0.001)	2.0	0.45	0.029
8	3.01	8.6	0.19	2.1	9.0	0.21
9	3.18	18 (± 2)	9.1 (± 0.5)	4.5	200	9.1
12	3.06	15	0.96	3.7	26	1.0
13	2.87	5.3 (± 1)	0.073 (± 0.004)	1.3	5.6	0.086
14	2.97	8.4	0.14	2.1	6.7	0.16
17	3.25	11	0.085	2.7	3.1	0.11
26	3.08	5.7	0.0043	1.4	0.31	0.018

*Selected specimens of series SC-C; cylindrical cores (2.54 × 2.54 cm) measured at room temperature and pressure. †Error in apparent magnetic susceptibility per unit volume (X_v) is ± 5 × 10^{-5} except where noted. ‡Error in natural remanent magnetization (NRM) is ± 2 in the least significant digit except where noted. §Induced magnetization (J) is calculated as $J = X_v \times H_{ext}$, where H_{ext} for Liberia is 24.9 A m^{-1}. ‖The Königsberger ratio (Q) is given by NRM × J^{-1}. ¶Total magnetization (M) is equal to NRM + J.

Native iron observed in the Liberian lower crustal granulites (Fig. 1) is in the multidomain (MD) size range (*23*); this allows an estimate, making magnetic susceptibility (*18, 24*), of <0.1 percent (by volume) Fe^0, making the assumption that only MD Fe^0 contributes to susceptibility. Even with this assumption, in accounting for the very large Hopkinson effect observed for pure iron (*25*) we find that the average induced magnetization of the granulites cannot be enhanced to 1 A m^{-1} or greater until depths equivalent to temperatures of 580° to 620°C are reached. Contrasts in total magnetization intensity of the granulites, however, range from 0.01 to 10 A m^{-1} at 25°C, and the highest intensities are due largely to NRM (Table 1).

Pure MD iron does not maintain a directionally stable magnetic remanence because the coercive force is ≃80 A m^{-1}, close to the magnitude of the earth's main field. Furthermore, the critical temperature of stable remanence (blocking temperature) in heating is usually a spectrum extending below the Curie point in MD materials. Moreover, magnetic minerals can acquire a viscous remanent magnetization parallel to an external field, particularly if exposed for long periods of time, even at temperatures below the blocking temperature. Thus, MD Fe^0 remanent magnetization in the lower continental crust could be largely aligned with the earth's field and would then be indistinguishable from induced magnetization when measured by high-altitude magnetic surveys.

We conclude that these native iron–bearing granulites are examples of the types of rocks that may be responsible for a significant part of the magnetization measured by POGO and MAGSAT satellite magnetometers and that the lower continental crust may be characterized by oxidation states equivalent to IW–

MW. Unless there is an intermediate relatively oxidized horizon, these oxidation states probably persist into the upper mantle and down through the depleted lithosphere (*26*); thus native iron may also exist below the Moho. If so, then it must be temperature and the αFe-γFe crystallographic phase boundary, rather than temperature and the αFe-γ^1Fe Curie point transition, that are the significant controls on the lower depth limit for iron ferromagnetism in the lithosphere. The αFe-γFe phase boundary (*27*) intersects the typical geothermal gradient of the continental shield at 75 to 80 km, but the deepest limit may be defined by a very low gradient geotherm—for example, the Sierra Nevada geotherm (*28*)—which intersects the αFe-γFe phase boundary at 90 to 95 km.

The granulites described here contain metallic iron, along with sulfides and graphite. These components, mitigated by grain contact and temperature (*29*), could contribute to the supposed high electrical conductivities of the lower crustal or upper mantle, explained (*30*) as being due to hydrous minerals or partial melting. The mafic granulite character, specific gravities, and the temperature, pressure, and V_{p} estimates correspond to model parameters (*31*) of the continental lower crust, but the extent to which native iron is present remains to be established, as does the precise mechanism that induced decomposition of iron-rich almandine garnet and ilmenite. Decomposition is not due directly to inclusion into the kimberlite because these gas-charged, CO_2-rich eruptives are moderately oxidizing and because mantle metasomatism is typically potassic (*32*), whereas the native iron–bearing granulite xenoliths are highly reduced and are sodium-enriched.

References and Notes

1. R. W. Kay and S. M. Kay, *Rev. Geophys. Space Phys.* **19**, 271 (1981); R. A. Kerr, *Science* **225**, 492 (1984); *ibid.* **224**, 1418 (1984).
2. E. R. Deutsch *et al.*, *Nature (London)* **269**, 684 (1977); A. K. Pedersen, *Contrib. Mineral. Petrol.* **69**, 397 (1979); P. Ramdohr, in *The Ore Minerals and Their Intergrowths* (Pergamon, New York, ed. 2, 1980), vol. 1, pp. 353–356.
3. F. M. Quodling, *J. Proc. R. Soc. N.S.W.* **97**, 81 (1964).
4. S. E. Haggerty, *J. Geophys. Res.* **87**, 10,811 (1982).
5. N. W. Rogers, *Nature (London)* **270**, 681 (1977).
6. H. R. Rollinson, *Lithos* **14**, 225 (1981).
7. D. J. Ellis and D. H. Green, *Contrib. Mineral. Petrol.* **71**, 13 (1979).
8. Freudenbergite is $Na_2Fe_2Ti_6O_{16}$ [G. Frenzel, *Neues Jahrb. Mineral. Monatsh.* **1**, 12 (1961)]. The ferrous iron analog has been reported by S. E. Haggerty [*ibid.* **8**, 375 (1983)] in Liberian granulites and by S. E. Haggerty and J. J. Gurney [*Eos* **65**, 305 (1984)] in high-pressure zircon-bearing nodules from kimberlites in South Africa.
9. Compositions are similar to those of scapolites described by A. P. Jones *et al.* [*J. Geol.* **91**, 143 (1983)]. On the basis of their conclusions and experimental data obtained by J. R. Goldsmith [*Geol. Soc. Am. Bull.* **87**, 161 (1976)], we can conclude that the scapolites of the Liberian granulites probably are stable only at relatively high pressures (12 to 20 kbar) at about 1000°C.
10. T. W. Bloxam and J. B. Allen, *Trans. R. Soc. Edinburgh* **64**, 1 (1960); B. E. Leake, *Mineral. Mag.* **38**, 389 (1971); B. L. Doolan, E. Zen, A. E. Bence, *Am. Mineral.* **63**, 1088 (1978).
11. L. C. Hsu, *J. Petrol.* **9**, 40 (1968); I. Keesman *et al.*, *Contrib. Mineral Petrol.* **31**, 132 (1971).
12. B. Simons and E. Woermann, *Contrib. Mineral. Petrol.* **66**, 81 (1978).
13. K. L. Spencer and D. H. Lindsley, *Am. Mineral.* **66**, 1189 (1981).
14. M. H. Manghnani, R. Ramananantoandro, S. P. Clark, Jr., *J. Geophys. Res.* **79**, 5427 (1974).
15. N. I. Christensen, *ibid.* **84**, 6849 (1979).
16. Analyses were conducted at $\approx$5°C min^{-1} and 1 to 100 mT in an argon atmosphere; we temperature-calibrated the data according to the procedure of S. D. Norem *et al.* [*Thermochim. Acta* **1**, 29 (1970)], utilizing the Curie point definition of M. Prévot *et al.* [*J. Geophys. Res.* **88**, 2316 (1983)].
17. P. Wasilewski and M. A. Mayhew, *Geophys. Res. Lett.* **9**, 325 (1982).
18. R. S. Carmichael, in *CRC Handbook of Physical Properties of Rocks*, R. S. Carmichael, Ed. (CRC Press, Boca Raton, Fla., 1982), vol. 2, chap. 2.
19. P. Wasilewski, H. H. Thomas, M. A. Mayhew, *Geophys. Res. Lett.* **6**, 541 (1979); P. Wasilewski and D. M. Fountain, *ibid.* **9**, 333 (1982).
20. G. Pullaiah *et al.*, *Earth Planet. Sci. Lett.* **28**, 133 (1975).
21. D. J. Dunlop, *J. Geophys.* **40**, 439 (1974).
22. S. E. Haggerty, *Can. J. Earth Sci.* **16**, 1281 (1979).
23. R. F. Butler and S. K. Bannerjee, *J. Geophys. Res.* **80**, 252 (1975).
24. L. J. Srnka and M. H. Mendenhall, *ibid.* **84**, 4667 (1979).
25. R. M. Bozorth, in *Ferromagnetism* (Van Nostrand, New York, 1951), p. 714.
26. S. E. Haggerty and L. A. Tompkins, *Nature (London)* **303**, 295 (1983).
27. P. W. Mirwald and G. C. Kennedy, *J. Geophys. Res.* **84**, 656 (1979).
28. A. H. Lachenbruch and J. H. Sass, in *The Earth's Crust—Its Nature and Physical Properties*, J. G. Heacock, Ed. [Geophysical Monograph Series, American Geophysical Union, Washington, D.C., 1977), vol. 20, pp. 626–675.
29. A. G. Duba and T. J. Shankland, *Geophys. Res. Lett.* **9**, 1271 (1982).
30. T. J. Shankland and M. E. Ander, *J. Geophys. Res.* **88**, 9475 (1983).
31. D. M. Fountain and M. H. Salisbury, *Earth Planet. Sci. Lett.* **56**, 263 (1981); A. G. Jones, *J. Geophys.* **49**, 226 (1981).
32. A. J. Erlank *et al.*, *Terra Cognita* **2**, 261 (1982).
33. Fieldwork was supported by the Weasua Mining and Development Corporation. Logistical support was provided by the Ministry of Lands, Mines, and Energy, Liberia, and by the embassies of the United States and the United Kingdom. NSF grant EAR83-08297 and NASA contract NAS5-26414 supported the analytical study.

23 August 1984; accepted 20 February 1985

Ecological Effects of Salicin at Three Trophic Levels: New Problems from Old Adaptations

Abstract. *Salicin, a toxic phenol glycoside, is used by larvae of the beetle* Chrysomela aenicollis *as a substrate for producing defensive secretions. In the east-central Sierra Nevada mountains of California, salicin concentrations ranged from 0.05 percent to over 5 percent of dry weight in leaves of different plants of* Salix orestera, *the Sierra willow. Beetles produced more secretion and suffered less predation on willows containing more salicin. In addition, leaf damage due to herbivory among 16 willow clones ranged from 0 to 20 percent of leaf area and was linearly related to salicin content. These results illustrate how a plant secondary chemical can become a problem for the plant when herbivores are adapted to use the chemical for their own benefit. The results also show the effect of a plant chemical on three trophic levels—the producer, a herbivore, and the predators of the herbivore.*

John T. Smiley
Jonathan M. Horn
Nathan E. Rank
Department of Ecology and
Evolutionary Biology,
University of California,
Irvine 92717, and White Mountain
Research Laboratory,
University of California

Secondary plant chemicals—those not necessary for primary metabolism—often serve as agents of plant defense, although they may solve other adaptive problems for plants as well (*1*). The repellent or toxic properties of these chemicals are well known (*2*) and have been shown to confer protection against herbivory under field conditions (*3*). Many insect herbivores effectively exploit secondary plant chemicals, using them to repel or poison their own predators (*4, 5*), to attract mates (*6*), and perhaps to exclude competitors (*7*). It is possible that some secondary plant chemicals are so useful to insect herbivores that the chemicals become a problem for the plant that produces them. Such a process may be very important in insect-plant coevolution, since it favors novel defensive compounds in plants and may thereby generate the tremendous diversity of compounds we see in present-day plants (*7, 8*). Here we report an increase in herbivory caused by salicin, a toxic phenol glycoside, in plants that produce large quantities of the compound. We also report the benefits of salicin for the herbivores under field conditions.

The evolution and ecology of salicin-exploiting chrysomelid beetles in the tribe Chrysomelini have been reported elsewhere (*9–12*). These beetles prefer food plants rich in salicin (primarily willows of the genus *Salix*), which is metabolized in dorsal glands to salicylaldehyde, which is stored and secreted by the glands, and glucose. The salicylaldehyde secretions are an effective deter-